Influence of Sea Surface Temperature on Humidity and Temperature in the Outflow of Tropical Deep Convection

ZHENGZHAO JOHNNY LUO,* DIETER KLEY,+,@ RICHARD H. JOHNSON,+ G. Y. LIU,* SUSANNE NAWRATH,# AND HERMAN G. J. SMIT@

* *Department of Earth and Atmospheric Sciences, and NOAA/CREST Center, City College of New York, CUNY, New York, New York*
+ *Department of Atmospheric Science, Colorado State University, Fort Collins, Colorado*
# *Klimahaus Betriebsgesellschaft mbH, Bremerhaven, Germany*
@ *Troposphäre, Institut für Energie- und Klimaforschung, Forschungszentrum Jülich, Jülich, Germany*

(Manuscript received 12 October 2010, in final form 14 July 2011)

ABSTRACT

Multiple years of measurements of tropical upper-tropospheric temperature and humidity by the Measurement of Ozone and Water Vapor by Airbus In-Service Aircraft (MOZAIC) project are analyzed in the vicinity of deep convective outflow to study the variations of temperature and humidity and to investigate the influence of the sea surface temperature (SST) on the outflow air properties. The principal findings are the following. 1) The distribution of relative humidity with respect to ice (RH_i) depends on where a convective system is sampled by the MOZAIC aircraft: deep inside the system, RH_i is unimodal with the mode at ~114%; near the outskirts of the system, bimodal distribution of RH_i starts to emerge with a dry mode at around 40% and a moist mode at 100%. The results are compared with previous studies using in situ measurements and model simulations. It is suggested that the difference in the RH_i distribution can be explained by the variation of vertical motions associated with a convective system. 2) Analysis of MOZAIC data shows that a fractional increase of specific humidity with SST, $q^{-1}\, dq/d\mathrm{STT}$, near the convective outflow is about 0.16–0.18 K^{-1}. These values agree well with previous studies using satellite data. Because MOZAIC measurements of temperature and humidity are independent, the authors further analyze the SST dependence of RH_i and temperature individually. Temperature increases with SST for both prevalent flight levels (238 and 262 hPa); RH_i stays close to constant with respect to SST for 238 hPa but shows an increasing trend for the 262-hPa level. Analysis conducted in this study represents a unique observational basis against which model simulations of upper-tropospheric humidity and its connection to deep convection and SST can be evaluated.

1. Introduction

It has long been realized that deep convection plays a key role in affecting the heat budget and moisture distribution of the tropics (Riehl and Malkus 1958). In recent years, the influence of tropical convection on the upper-troposphere moisture has received increased attention because of its important role in climate feedback (Lindzen 1990; Held and Soden 2000; Sherwood et al. 2010). The tropical upper troposphere is connected to near-surface air by deep convection, whereby air from close to the surface is lifted to the upper troposphere. Outside of the deep convective region air generally experiences gentle subsidence due to the radiative cooling of the atmosphere, so the upper troposphere of the nonconvective regions does not feel much of an influence from the surface immediately below. A number of previous studies have investigated how upper-tropospheric temperature and humidity are affected by the variation of the sea surface temperature, which is often taken as evidence for the upper-tropospheric water vapor feedback (Minschwaner and Dessler 2004; Gettelman and Fu 2008; Chuang et al. 2010). Instead of using the whole-tropics mean SST, previous investigators usually used SST over regions whose rain rates exceed a certain threshold (Chuang et al. 2010), or outgoing longwave radiation (OLR) is smaller than some prescribed values (Minschwaner and Dessler 2004). This reflects the understanding that it is within the deep convective region

Corresponding author address: Dr. Zhengzhao Johnny Luo, Department of Earth and Atmospheric Sciences, and NOAA/CREST Center, City College of New York, CUNY, New York, NY 10031. E-mail: luo@sci.ccny.cuny.edu

DOI: 10.1175/2011JCLI4124.1

that near-surface air directly communicates its influence to the upper troposphere.

The influence of SST on the upper-tropospheric air properties near convective outflow can also be understood through a new conceptual paradigm that has recently been established to explain the distribution of tropical upper-tropospheric humidity (UTH), that is, the so-called advection–condensation model (Sherwood 1996; Pierrehumbert and Roca 1998; Dessler and Sherwood 2000; Pierrehumbert et al. 2007; Sherwood et al. 2010). The essence of the ''advection–condensation'' model is conservation of specific humidity (q) along a Lagrangian trajectory: since q remains conserved in the absence of sources or sinks, its value at a particular location in the free troposphere is simply determined by the lowest saturation value that the air parcel has experienced since its departure from the boundary layer. According to this model, the distribution of UTH can be viewed, in a Lagrangian perspective, as being controlled largely by two factors: the ''last saturation point'' (usually where air leaves the convective region in outflows) and the subsequent 3D wind field. The influence of SST on the last saturation point can be studied by examining the SST dependence of air properties near the convective outflow, and this influence will be felt, through subsequent advection, by much of the tropics that are nonconvective. In this study, we investigate the influence of SST on humidity and temperature in the outflow of tropical deep convection using a unique dataset—Measurement of Ozone and Water Vapor by Airbus In-Service Aircraft (MOZAIC)—with multiple years of high-quality, in situ measurements near tropical deep convection. If there is a feedback mechanism based on the coupling between upper-tropospheric water vapor and the SST through deep convection, it should be manifested in a dependence of humidity near convective outflow on the underlying SST.

Another topic investigated in this study is the relative humidity (RH) of outflowing air from deep convection. It is often implicitly assumed that RH with respect to the ice phase (RH_i) is saturated (100%) in convective outflow, as is the case in simplified models such as the advection–condensation model. However, this is an experimentally unproven assumption. Recent discovery of frequent occurrence of ice supersaturation in the upper troposphere, both inside and outside of clouds, has cast further doubt upon this assumption[1] (e.g., Gierens et al. 2000; Jensen et al. 2001; Peter et al. 2008; Luo et al. 2007; Krämer et al. 2009; among others). Satellite measurements face two major difficulties in answering this question: 1) extensive opaque clouds near deep convection often prevent accurate retrieval of humidity and 2) the vertical resolution of satellite instruments is coarse, further affecting the accuracy of retrieval in view of the fact that specific humidity changes rapidly with height. The two most advanced satellite-borne instruments that measure the upper tropospheric humidity (UTH) are the Atmospheric Infrared Sounder (AIRS) on board *Aqua* and the Microwave Limb Sounder (MLS) on board *Aura*, flying in formation as members of the A-Train constellation (Stephens et al. 2002). AIRS UTH measurements are limited to where the effective cloud fraction over a 45 km $\times$ 45 km area is lower than 70%–80% (Susskind et al. 2006; Gettelman et al. 2006), whereas MLS retrieval is affected by scattering due to large ice particles (Wu et al. 2006), a situation that is often encountered near deep convective outflow. The vertical resolution for AIRS measurements of specific humidity and temperature is approximately 2–3 km (Maddy and Barnet 2008); MLS mainly suffers from coarse horizontal resolution ($\sim$165 km) owing to the limb sounding geometry (Livesey et al. 2006). Fetzer et al. (2008) provided a detailed comparison of upper-tropospheric water vapor (UTWV) measured by the two instruments. Operational radiosondes are another potential source of UTH measurements; however, they lose accuracy and precision at temperatures lower than -40°C (Elliot and Gaffen 1991; Wang et al. 2003) and may be expelled from rapidly ascending air or even destroyed if the balloon gets close to the convective core. Research aircraft carrying research-type humidity instrumentation should, in principle, provide high quality data. Indeed, the prevalence of ice supersaturation in the upper troposphere was first established by these high-accuracy aircraft measurements, and a recent study by Krämer et al. (2009) conducted a comprehensive analysis of aircraft observations contrasting RH_i inside and outside cirrus. Nevertheless, the campaign-style aircraft measurements are generally very limited in space and time. Most of them do not fly close to convective systems to sample the outflow air [with a notable exception of the Cirrus Regional Study of Tropical Anvils and Cirrus Layers–Florida-Area Cirrus Experiment (CRYSTAL-FACE; www.espo.nasa.gov/crystalface/index.html)].

In this study, we draw upon a unique data source from the MOZAIC project that collects high-quality (5%–7%) and long-term (over 10 years) measurements of temperature, water vapor, and other trace gases from instruments on board commercial aircraft. Oftentimes commercial aircraft have to fly through deep convective

[1] An international workshop was held in Karlsruhe, Germany, on 12–15 June 2007 to specifically address the subject of ice supersaturation in the upper troposphere; the workshop report (Peter et al. 2008) summarizes our current understanding of the problem based on field observations, laboratory work, modeling, and theoretical studies.

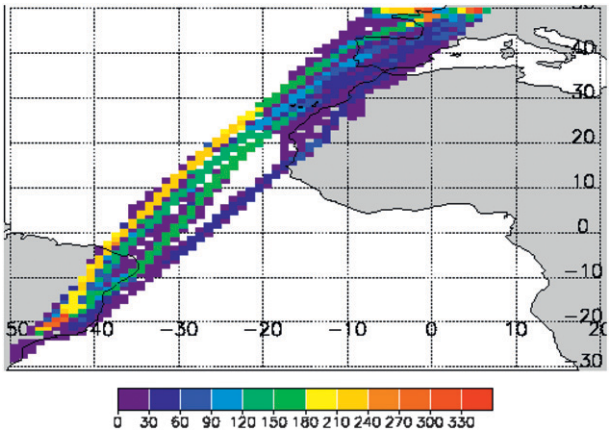

FIG. 1. Number of flights in bins of 1° latitude × 1° longitude from September 1994 to April 2000. Our analysis in this study is limited to 0°–10°N.

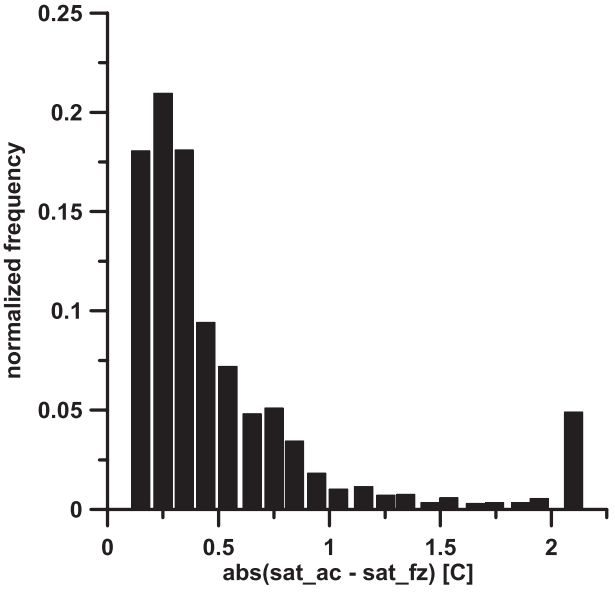

FIG. 2. Normalized number of observations of absolute differences between two temperature sensors, each on three different aircraft.

clouds, especially when crossing the ITCZ (although pilots usually try to avoid convective cores). An unfortunate example was the Air France 477 en route from Rio de Janeiro to Paris that crashed inside a convective system over the tropical Atlantic in June 2009. One of the airlines that carries the MOZAIC instrument is Air France, and this route from Brazil to Europe is exactly where our data are collected for this study. Multiple years of MOZAIC data thus become a valuable source for answering the questions raised above. Specifically, we report humidity measurements from MOZAIC in close proximity to deep convection over the tropical Atlantic Ocean and investigate their dependence on SST. (Section 2 describes how we decide whether a measurement is made near convective outflow). Figure 1 shows the flight corridor. The data cover the period from September 1994 to April 2000.[2] To stay close to the convective zone of the tropical Atlantic, we limit our analysis to the latitude band 0°–10°N (see Fig. 1). Over this region, SST for the identified convective cases varies temporally and spatially by ~3°C.

2. Data description and analysis method

MOZAIC is a project for which passenger aircraft are equipped with accurate semiautomatic sensors that, in phase 1 from 1994 to 2003, measured relative humidity (RH), temperature (T), and ozone on scheduled flights (Marenco et al. 1998). Specific humidity (q) is calculated from RH and T. Relative humidity is measured at cruise level with a total uncertainty of 5%–7% RH. Details on the water vapor instrumentation can be found in Helten et al. (1998, 1999). Temperature is measured with two sensors: 1) a platinum resistance thermometer, packed together with the humidity-sensing device inside a Rosemount B102 housing, approximately 7 m aft from the aircraft nose and 2) the thermometer of the aircraft, located near the housing. Both thermometers have a nominal accuracy of 0.2°C. Due to adiabatic compression, the measured dynamic temperature is about 30°C higher than the static atmospheric temperature. Both temperature sensors, after conversion to static temperature, usually agree to within a few tenths of a degree. However, probably owing to a fast change of the aircraft's angle of attack or turbulence, larger deviations were sometimes observed. Figure 2 shows the histogram of the differences of the two temperature sensors in the tropical Atlantic region from 1994 to 2000 when MOZAIC aircraft were within 100–200 km of deep convection. It shows that the two sensors occasionally exhibited differences greater than 2 K: altogether there were 115 events out of a total of 2347 with differences greater than 2 K. Those differences were randomly distributed between 2 and 17 K. Those events have been lumped together and are shown at 2.1 K in Fig. 2. To screen out these data, all measurements of RH and T where the two temperature sensors differ by more than 0.5°C have been discarded. Under these precautions the uncertainty of the temperature measurement is close in value to the uncertainty of $T \approx 0.5$°C, as already given in Helten et al. (1998). Dynamic relative humidity (RH_d) is measured directly

[2] After 2000, MOZAIC aircraft were often deployed to fly outside of the tropical Atlantic region. Note that it is entirely up to the airlines to decide which routes these commercial aircraft fly.

and converted to static relative humidity using the temperature sensor in the humidity Rosemount housing (Helten et al. 1998). At an uncertainty of 0.5° of the temperature sensor, the accuracy of the humidity sensor is not adversely affected. The time resolution of the MOZAIC humidity measurements in the upper troposphere is 1 min, which, at cruising speed, corresponds to a spatial resolution of about 15 km. In the tropical regions, MOZAIC aircraft at cruising altitude fly at five discrete pressure levels: 288, 262, 238, 217, and 197 hPa (about 10–12 km). Over the tropical Atlantic, the most prominent flight levels are 238 and 262 hPa.

In support of the MOZAIC project, Météo-France, the French weather service, calculated 3D back trajectories (based on European Centre for Medium-Range Weather Forecasts analysis winds at the spatial and temporal resolutions of 0.5° and 6 h) starting from the location of each MOZAIC measurement and tracing backward in time for two days. This helps diagnose how far a sampled air parcel (by MOZAIC) has traveled from the originating convection. A number of ways could be utilized to identify deep convective clouds from satellite. Here we use cloud-top temperature (CTT) inferred from IR sensors because of its availability both day and night. Specifically, we use the European Organisation for the Exploitation of Meteorological Satellites (EUMETSAT) Climate Data Set (CDS) (EUMETSAT 1999). The raw satellite data (Meteosat) have pixels of 5 km × 5 km; however, EUMETSAT CDS groups them into segments, each consisting of 32 × 32 pixels (i.e., 160 km × 160 km). Each segment is then divided into up to five clusters corresponding to areas with discrete optical properties or clouds of different altitude ranges. We first define the deep convective region as CDS segments that have CTT < 240 K. The convective origin of a MOZAIC measurement is identified by searching backward along each trajectory until a deep convective segment is encountered, following Nawrath (2002). To ensure a MOZAIC measurement was, indeed, made within the vicinity of deep convection outflow, we further impose the following stringent conditions: 1) back trajectories indicate zero time ($t = 0$) from the MOZAIC measurement to the segment containing deep convection, 2) deep convective clouds (i.e., CTT < 240 K) cover 100% of the segment, and 3) CTT $\leq T_{AC}$, where T_{AC} is the temperature at the aircraft altitude. The last condition requires that deep convective clouds extend to above the aircraft flight level (200–300 hPa). Since most of the T_{AC} at the cruise level is <230 K, we actually require that CTT be much colder than the 240-K threshold. Admittedly, use of CTT could select high-level clouds of nonconvective nature (such as cirrus formed in situ). However, the aforementioned three conditions make this highly unlikely. As shown by Luo and Rossow (2004), tropical cirrus that form in situ well away from deep convection are usually optically thin (optical thickness <1) and semitransparent. As such, the IR-derived CTTs have a significant warm bias (usually >260 K). Hence, to have CTT < 240 K throughout the whole 160 km × 160 km regions, clearly indicates the presence of deep convection and associated cirrus anvils (i.e., convective outflow). Our visual examination of satellite images also supports this conclusion.

SST data used in this study are from the Reynolds weekly average, 1° latitude/longitude SST dataset (Reynolds et al. 2002). They are obtained from the Columbia University International Research Institute (IRI) for Climate and Society Data Library. We use linear interpolation in time to get the SST for the time of each MOZAIC observation. There is some uncertainty in using weekly averaged SST to represent the surface condition associated with deep convection because large convective systems can create mesoscale SST anomalies (e.g., Soloviev et al. 2002). Indeed, most cases analyzed in this study show that SST tends to be slightly colder a few days after the convection than a few days before (note that the Reynolds weekly SST data are centered on Wednesdays during 1996–2000). This suggests that convection cools the ocean surface. Nevertheless, using temporal interpolation between two bracketing Wednesdays will partially alleviate this problem.

3. Relative humidity near convective outflow

Histograms of relative humidity over ice (RH_i) in the outflow of deep convection ($t = 0$) are presented in Fig. 3 (top panel). Only data from the 238-hPa cruise level is shown. The humidity distribution is unimodal with a most likely RH_i at 114%: a similar result was also noted in Kley et al. (2007). The unimodal distribution remains as we gradually relax the cold cloud coverage to lower values (i.e., lower than 100% cloud cover). The only change is that the RH_i mode shifts to slightly lower values (110%). However, when the segmental coverage with cold clouds was lowered to below 70%, bimodality starts to emerge. The bottom panel of Fig. 3 shows a histogram of RH_i for cold cloud coverage lower than 30% (but $t = 0$ still holds): it shows a dry mode at around 40% and a moist mode, now at about ice saturation (100%). The bimodal distribution as shown in the bottom panel in Fig. 3 is similar to that observed by Zhang et al. (2003), who attributed the two modes to two key processes controlling UTH, namely, convective moistening and subsidence drying.

The different RH_i distributions, as shown in Fig. 3, can be understood as aircraft sampling different areas in

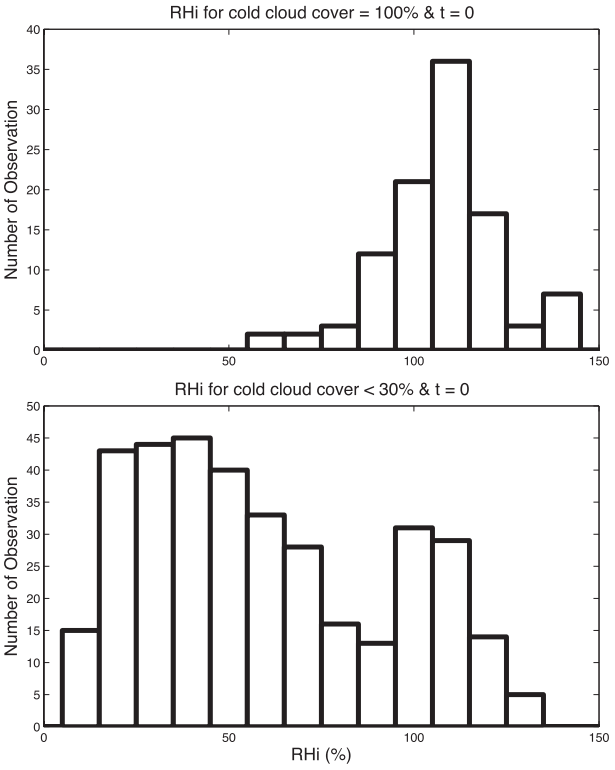

FIG. 3. Histogram of RH_i at 238 hPa for (top) cold cloud coverage = 100% and (bottom) cold cloud coverage < 30%. For both cases MOZAIC observations were made near convective outflow (back trajectory $t = 0$).

the vicinity of convective systems. Recall that inside of a given segment of the CDS data (160 km × 160 km), a single convective pixel (5 km × 5 km) with a sufficiently low cloud-top temperature suffices to stop the back trajectory search and label the segment as the convective origin ($t = 0$). For the cases that have cold cloud coverage equal to 100% (Fig. 3a), the MOZAIC measurements were most likely made deep inside a convective system. Otherwise, it would be hard to see all of the 160 km × 160 km area covered with IR-derived CTT < 240 K; cirrus formed in situ tend to have a warm IR brightness temperature, as shown in Luo and Rossow (2004). For the cases where cold cloud coverage is <30% (and $t = 0$), the flights were probably just bordering the convective system.[3] In the next section (section 4), which focuses on the influence of SST on air property in the convective outflow, we exclude measurements that are shown in the bottom panel of Fig. 3 (because we are not certain that these data were actually collected in close proximity of deep convection), and limit our analysis to cases with cold cloud coverage = 100% only.

The finding that the RH_i mode is 114% deep inside convective outflow but drops to 100% in the outskirts of a convective system deserves further discussion. It is well understood that, in the case of scarcity of ice nuclei, ice supersaturation can be achieved in the cold upper troposphere until RH_i exceeds the homogeneous freezing threshold. Once this threshold is reached and ice particles start to form, they will consume moisture and reduce the humidity level back to a dynamical equilibrium. Krämer et al. (2009) used an observation-based model to study the dynamical equilibrium of cirrus clouds. According to their model, the relaxation time to bring RH_i back to dynamical equilibrium depends on a number of factors, including ice particle size, number density, temperature, and vertical velocity, but is generally on the order of a few minutes to tens of minutes. The dynamical equilibrium value for RH_i also varies with these factors, with vertical velocity playing a particularly important role. For temperatures relevant to the MOZAIC measurements (~230 K), the dynamical equilibrium RH_i is close to 100% for low vertical velocity, $O(1\ \text{cm s}^{-1})$, but reaches ~110% for high vertical velocity $O(1\ \text{m s}^{-1})$. If we assume the most frequent RH_i value from MOZAIC measurements—namely, the mode as shown in Fig. 3—represents the observational equivalent of the dynamical equilibrium RH_i (i.e., assuming multiple years of aircraft measurements do not favor any transient state), Fig. 3 can be interpreted as suggesting that 1) relatively large vertical velocity $O(1\ \text{m s}^{-1})$ prevails deep inside convective outflow where RH_i mode is at ~114% and 2) vertical velocity becomes much smaller $O(1\ \text{cm s}^{-1})$ toward the fringe of the convective system where RH_i mode is close to 100%. This interpretation is consistent with our general understanding of the vertical motions associated with a mesoscale convective system (e.g., Houze 1993): mesoscale updraft dominates the regions near stratiform precipitation (which is connected to convective cores that aircraft try to avoid) and the vertical motion starts to taper off as we move away from the center of the convective system. Another factor that affects RH_i is mixing: moving away from the convective cores, there is more opportunity for outflowing air to mix with the surroundings, which reduces RH_i, although this effect is difficult to quantify. Finally, we note that vertical velocity $O(1\ \text{m s}^{-1})$ is unlikely seen in cirrus of nonconvective origin. For the cirrus cases collected by Krämer et al. (2009), where the RH_i mode is close to 100% (except at temperatures colder than 205 K where the nucleation process is extremely slow), they are

[3] It should be admitted that this interpretation holds best in a statistical sense. The next paragraph, which discusses possible reasons for the difference in RH_i distribution, seems to lend support to this interpretation.

probably cirrus of nonconvective origin or in situ cirrus that has smaller vertical velocity. Luo and Rossow (2004) showed that more than half of the tropical cirrus form in situ well away from convection. Hence, our analysis here complements previous aircraft studies in the sense that it presents an observation of relative humidity in a vigorously convecting environment. At the other main cruise level (262 hPa), very similar results (not shown) were obtained.

4. SST dependence of upper-tropospheric temperature and humidity near convective outflow

Deep convection is an effective channel through which near-surface air directly communicates its influence to the upper troposphere. Because of the short time scale for convection (on the order of 1 h), certain variables such as equivalent potential temperature (θ_e) and moist static energy (MSE) are nearly conserved (apart from freezing effects), so we expect that air in the convective outflow shares some of the signatures of the near-surface air [although entrainment of the environment air can dilute the surface influence, Kley et al. (2007)]. Hence, we expect that SST has some influence on the air properties within convective outflow. This influence will then be passed on to the rest of the tropics (most of which are not actively convecting) through the large-scale circulation. In this section, we investigate how upper-tropospheric temperature and humidity near the convective outflow are related to the SST. We focus on the two prevalent cruise levels—238 and 262 hPa. MOZAIC aircraft fly less frequently on the other three levels, so too few cases are found there and no statistically robust conclusion can be drawn for them.

For the 238-hPa level, a total of 106 data points pass the stringent selection conditions for being near convective outflow (see section 2 for details). The 262-hPa level has 90 data points. The corresponding SST ranges from 299.3 to 302.1 K. This is consistent with previous findings by Graham and Barnett (1987), Waliser and Graham (1993), and others, who found that deep convection over the tropical ocean is predominantly confined to areas with SST $\geq$ 299.5 K. Figures 4–6 show the 238-hPa RH_i, specific humidity q, and temperature T, plotted versus the collocated SST. The logarithm of specific humidity is shown such that the regression slope represents the fractional change, that is, $q^{-1}dq/d\mathrm{STT}$. Linear least squares fits with regression uncertainty (95% confidence limit) are also shown in the figures.

To put the discussion of these relationships in a relevant context, we consider the Clausius–Clapeyron relation, which gives

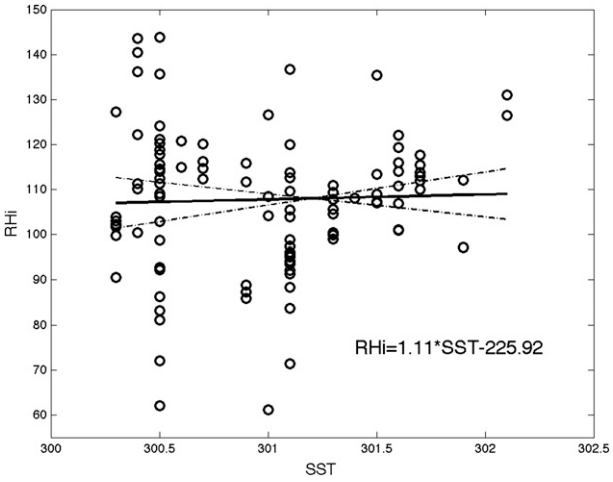

FIG. 4. Scatterplot of RH_i for cruise level 238 hPa near convection ($t = 0$) against the collocated SST. Linear least squares fits with uncertainty (95% confidence limit) are also shown.

$$\frac{d\mathrm{RH}_i}{d\mathrm{SST}} = \mathrm{RH}_i\frac{1}{q}\frac{dq}{d\mathrm{SST}} - \mathrm{RH}_i\frac{L}{RT^2}\frac{dT}{d\mathrm{SST}}, \qquad (1)$$

where L is the latent heat of sublimation (2.83×10^6 J kg^{-1}) and R is the gas constant for water vapor (461.5 J K^{-1} kg^{-1}). Figure 4 shows that RH_i does not change much with SST. The slight increasing trend ($1.1 \pm 3.1\%$ RH_i K^{-1}) is not statistically significant; it goes from small negative values (-2.0% RH_i K^{-1}) to small positive values (4.2% RH_i K^{-1}) when the standard deviation of the slope (shown as the dashed lines in Fig. 4) is considered. In contrast, both q and T increase with SST (Figs. 5 and 6, also see Table 1 for numerical values). The increase in rates for $q^{-1}dq/d\mathrm{STT}$ and $dT/d\mathrm{SST}$, as derived from the linear regressions, are 0.18 ± 0.033 K^{-1} and 1.4 ± 0.16 K K^{-1}, respectively. Substituting these values into Eq. (1) and using the average RH_i (108%) and T (229.5 K), we obtain the first term on the rhs of Eq. (1), namely,

$$\mathrm{RH}_i\frac{1}{q}\frac{dq}{d\mathrm{SST}},$$

as 19.4% RH_i K^{-1} and the second term,

$$\mathrm{RH}_i\frac{L}{RT^2}\frac{dT}{d\mathrm{SST}},$$

as 17.2% RH_i K^{-1}. The left-hand side, $d\mathrm{RH}_i/d\mathrm{SST}$, is thus equal to $19.4\% - 17.2\% = 2.2\%$ RH_i K^{-1}. This is somewhat different from the observed value through linear regression, which is 1.1% RH_i K^{-1}. But this difference should be interpreted in a proper context: 1) the nonlinear effect is ignored in the calculation above; that is, we use the linear averages of RH_i and T in evaluating

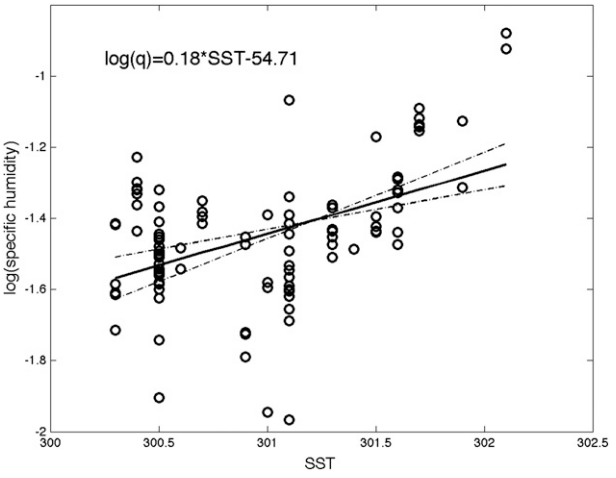

FIG. 5. Scatterplot of specific humidity q (in natural logarithm) for cruise level 238 hPa near convection ($t = 0$) versus the collocated SST. Linear least squares fits with uncertainty (95% confidence limit) are also shown.

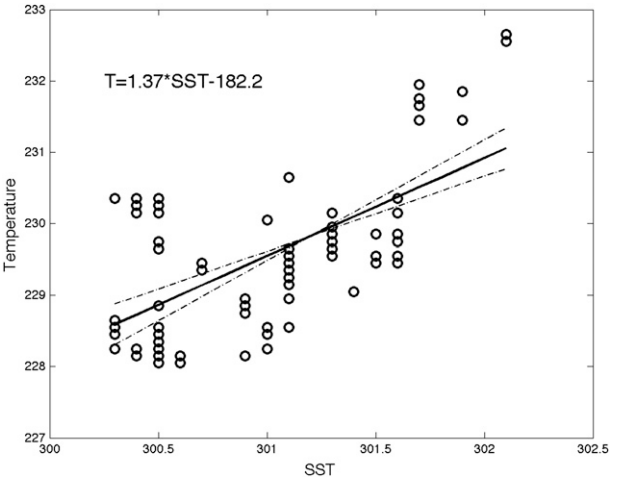

FIG. 6. Scatterplot of temperature observations (kelvin) for cruise level 238 hPa near convection ($t = 0$) against the collocated SST. Linear least squares fits with uncertainty (95% confidence limit) are also shown.

Eq. (1), which could introduce some errors. 2) The error bar for $d\mathrm{RH}_i/d\mathrm{SST}$ is 3.1% $\mathrm{RH}_i\ \mathrm{K}^{-1}$, so the observed $d\mathrm{RH}_i/d\mathrm{SST}$ ranges from $-2.0_{\ i}$ to 4.2% $\mathrm{RH}_i\ \mathrm{K}^{-1}$. In light of these uncertainties, we thus consider our calculation based on the Clausius–Clapeyron relation (2.2% $\mathrm{RH}_i\ \mathrm{K}^{-1}$) not significantly different from the observed value (1.1% $\mathrm{RH}_i\ \mathrm{K}^{-1}$). Note that $d\mathrm{RH}_i/d\mathrm{SST}$ is just a small residual of two large numbers that are about one order of magnitude greater.

The increase rate of q with SST, as derived from MOZAIC (0.18 K^{-1}), is very similar to that by Chuang et al. (2010), who used AIRS data to show that $q^{-1}dq/d\mathrm{STT}$ is ~0.18 K^{-1} for the 250-hPa level, although they use the whole-tropics averaged q (but SST is from the average over convective regions), while our analysis is done locally in the vicinity of deep convective outflow. Su et al. (2006) analyzed tropical upper-tropospheric water vapor data in terms of column integration between 316 and 147 hPa from the MLS on board the *Aura* satellite and found that, for SST $\geq$ 300 K, $d\ \ln(\mathrm{H_2O})/d\mathrm{SST} = 0.17\ \mathrm{K}^{-1}$, where $\mathrm{H_2O}$ refers to the column-integrated water vapor mass. So, in situ measurements from MOZAIC corroborate previous studies using satellite data.[4] Moreover, with independent in situ measurements of temperature and humidity from MOZAIC, we are able to further decompose the SST dependence of the relative humidity to those due to changes in specific humidity and temperature. For satellite retrieval, however, temperature and humidity signals are always entangled in the radiative transfer equation (i.e., the Schwarzchild equation).

Analysis for the 262-hPa level gives similar $q^{-1}dq/d\mathrm{STT}$: ~0.16 (see Table 1 for a summary of SST dependence of temperature and humidity for the two prevalent cruise levels). However, temperature increases with SST at a somewhat slower rate than that at the 238-hPa level (0.69 $\mathrm{K\ K}^{-1}$), resulting in a larger $d\mathrm{RH}_i/d\mathrm{SST}$ at about 8.8% $\mathrm{RH}_i\ \mathrm{K}^{-1}$. It is not immediately clear to us what accounts for the differences between the 262- and 238-hPa levels. Especially puzzling is $dT/d\mathrm{SST} < 1$ for the 262-hPa level. Undiluted moist adiabatic ascent should produce $dT/d\mathrm{SST} > 1$. A few possible reasons could account for the small $dT/d\mathrm{SST}$: 1) uncertainties in collocated SST; 2) entrainment of environment air during ascent, which may dilute the SST influence; and 3) measurements being made not close enough to the convective cores, thus allowing mixing with ambient air. Since there are only 90 data points for the 262-hPa level, it is possible that these errors affect our results. When more data points are collected by MOZAIC in the future, we will revisit the problem.

TABLE 1. Dependence of T, RH_i, and q on SST for two prominent flight levels (238 and 262 hPa). The numbers in the parenthesis are 95% confidence intervals for the regressed slopes.

	$dT/d\mathrm{SST}$ (K^{-1} K)	$d\mathrm{RH}_i/d\mathrm{SST}$ (% K^{-1})	$q^{-1}dq/d\mathrm{STT}$ (K^{-1})
238 hPa	1.4 (0.16)	1.1 (3.1)	0.18 (0.033)
262 hPa	0.69 (0.13)	8.8 (3.4)	0.16 (0.037)

[4] One note of caution is that previous satellite studies examined q variations over the whole tropics (although they only use SST over convective regions), whereas our analysis is confined to near convective outflow. Since satellites have a more complete spatial/temporal coverage, a future study can be planned to analyze satellite data the same way as was done with MOZAIC.

5. Conclusions and discussion

Tropical deep convection plays a critical role in communicating the influence of the surface to the upper troposphere. If there is a feedback mechanism based on the coupling between upper-tropospheric water vapor and the SST through convection, it should be manifested in a dependence of humidity near convective outflow on the underlying SST. One purpose of this work is to study the variations of the upper-tropospheric humidity in the vicinity of deep convection and to investigate the influence of SST on air properties in the outflow of deep convection using a unique dataset, Measurement of Ozone and Water Vapor by Airbus In-Service Aircraft (MOZAIC). Another subject investigated is the distribution of relative humidity in convective outflow. It is often implicitly assumed that relative humidity with respect to the ice phase (RH_i) is saturated (100%) in convective outflow, as in some simplified models. Recent discovery of the frequent occurrence of ice supersaturation in the upper troposphere casts doubt upon this assumption. While previous aircraft measurements investigated the distribution of RH_i inside cirrus clouds, no particular attention has been paid to deep convective outflow where air motions are more vigorous than most cirrus cases, especially those cirrus that form in situ away from convection. The main findings are summarized as follows:

1) The distribution of relative humidity with respect to ice depends on where a convective system is sampled by the MOZAIC aircraft: deep inside the system, RH_i is unimodal with the mode at ~114% (i.e., supersaturated); near the outskirts of the system, a bimodal distribution of RH_i starts to emerge with a dry mode at around 40% and a moist mode at about 100%. We compare our results with previous studies using in situ measurements and model simulations. It is suggested that the difference in RH_i distribution can be explained by the variation of vertical motions associated with a convective system from the center to the fringe.
2) The fractional increase of specific humidity with SST, $q^{-1}dq/d\mathrm{STT}$, is 0.16–0.18 for two prevalent cruise levels (262 and 238 hPa). These values agree well with previous studies using satellite data. Moreover, since MOZAIC makes independent measurements of temperature and humidity, we further analyze the SST dependence of RH_i and temperature individually. Temperature increases with SST for both prevalent flight levels (238 and 262 hPa); RH_i stays close to constant with respect to SST for the 238-hPa level but shows an increasing trend for the 262-hPa level.

This is the first time, to our knowledge, that long-term and high-accuracy aircraft measurements of humidity have been utilized to study the moisture distribution and its SST dependence in the vicinity of *tropical deep convective flow*. Analysis conducted in this study helps clarify some relationships as seen from satellites. It also represents a unique observational basis against which GCM simulations of upper-tropospheric humidity and its connection to deep convection and SST can be evaluated. Our ongoing research seeks to match MOZAIC measurements with advanced satellite cloud products (e.g., CloudSat) to better understand the relation between UTH and convective properties.

Acknowledgments. This work was partially supported by the National Science Foundation (NSF) under Grant ATM-0444244 and Forschungszentrum Jülich, and partially supported by NOAA Grant NA10NES4400004, which was awarded to City College of New York, and NASA MAP Grant NNX09AJ46G, which was awarded to the University of Michigan. We thank Gert König-Langlo from the Alfred Wegener Institute for supplying R/V *Polarstern* data. The lead author wishes to thank Dr. Xianglei Huang of the University of Michigan for his helpful discussion.

REFERENCES

Chuang, H., X. Huang, and K. Minschwaner, 2010: Interannual variations of tropical upper tropospheric humidity and tropical rainy-region SST: Comparisons between models, reanalyses, and observations. *J. Geophys. Res.,* **115,** D21125, doi:10.1029/2010JD014205.

Dessler, A. E., and S. C. Sherwood, 2000: Simulations of tropical upper tropospheric humidity. *J. Geophys. Res.,* **105,** 20 155–20 184.

Elliot, W. P., and D. J. Gaffen, 1991: On the utility of radiosonde humidity archives for climate studies. *Bull. Amer. Meteor. Soc.,* **72,** 1507–1520.

EUMETSAT, 1999: Meteosat archive user handbook, issue 2.2. EUMETSAT.

Fetzer, E. J., and Coauthors, 2008: Comparison of upper tropospheric water vapor observations from the Microwave Limb Sounder and Atmospheric Infrared Sounder. *J. Geophys. Res.,* **113,** D22110, doi:10.1029/2008JD010000.

Gettelman, A., and Q. Fu, 2008: Observed and simulated upper-tropospheric water vapor feedback. *J. Climate,* **21,** 3282–3289.

——, E. J. Fetzer, A. Eldering, and F. W. Irion, 2006: The global distribution of supersaturation in the upper troposphere from the Atmospheric Infrared Sounder. *J. Climate,* **19,** 6089–6103.

Gierens, K., U. Schumann, M. Helten, and H. Smit, 2000: Ice-supersaturated regions and subvisible cirrus in the northern midlatitude upper troposphere. *J. Geophys. Res.,* **105** (D18), 22 743–22 753.

Graham, N. E., and T. P. Barnett, 1987: Sea surface temperature, surface wind divergence, and convection over tropical oceans. *Science,* **238,** 657–659.

Held, I. M., and B. J. Soden, 2000: Water vapor feedback and global warming. *Annu. Rev. Energy Environ.,* **25,** 441–475.

Helten, M., H. G. J. Smit, W. Sträter, D. Kley, M. Zöger, R. Busen, and P. Nedelec, 1998: Calibration and performance of automatic compact instrumentation for the measurement of relative humidity from passenger aircraft. *J. Geophys. Res.,* **103,** 25 643–25 652.

——, and Coauthors, 1999: In-flight intercomparison of MOZAIC and POLINAT water vapor measurements. *J. Geophys. Res.,* **104,** 26 087–26 096.

Houze, R. A., Jr., 1993: *Cloud Dynamics*. Academic Press, 573 pp.

Jensen, E. J., and Coauthors, 2001: Prevalence of ice-supersaturated regions in the upper troposphere: Implications for optically thin ice cloud formation. *J. Geophys. Res.,* **106** (D15), 17 253–17 266.

Kley, D., H. G. J. Smit, S. Nawrath, Z. Luo, P. Nedelec, and R. H. Johnson, 2007: Tropical Atlantic convection as revealed by ozone and relative humidity measurements. *J. Geophys. Res.,* **112,** D23109, doi:10.1029/2007JD008599.

Krämer, M., and Coauthors, 2009: Ice supersaturations and cirrus cloud crystal numbers. *Atmos. Chem. Phys.,* **9,** 3505–3522.

Lindzen, R. S., 1990: Some coolness concerning global warming. *Bull. Amer. Meteor. Soc.,* **71,** 288–299.

Livesey, N. J., W. V. Snyder, W. G. Read, and P. A. Wagner, 2006: Retrieval algorithms for the EOS Microwave Limb Sounder (MLS) instrument. *IEEE Trans. Geosci. Remote Sens.,* **44,** 1144–1155.

Luo, Z., and W. B. Rossow, 2004: Characterizing tropical cirrus life cycle, evolution, and interaction with upper-tropospheric water vapor using Lagrangian trajectory analysis of satellite observations. *J. Climate,* **17,** 4541–4563.

——, D. Kley, R. H. Johnson, and H. Smit, 2007: Ten years of measurements of tropical upper-tropospheric water vapor by MOZAIC. Part I: Climatology, variability, transport, and relation to deep convection. *J. Climate,* **20,** 418–435.

Maddy, E. S., and C. D. Barnet, 2008: Vertical resolution estimates in version 5 of AIRS operational retrievals. *IEEE Trans. Geosci. Remote Sens.,* **46,** 2375–2384.

Marenco, A., and Coauthors, 1998: Measurement of ozone and water vapor by Airbus in-service aircraft: The MOZAIC airborne program, an overview. *J. Geophys. Res.,* **103,** 25 631–25 642.

Minschwaner, K., and A. E. Dessler, 2004: Water vapor feedback in the tropical upper atmosphere: Model results and observations. *J. Climate,* **17,** 1272–1282.

Nawrath, S., 2002: Water vapor in the tropical upper troposphere: On the influence of deep convection. Ph.D. thesis, Universität zu Köln, 104 pp. [Available online at http://kups.ub.uni-koeln.de/volltexte/2003/411/.]

Peter, T., M. Krämer, and O. Möhler, 2008: Upper tropospheric humidity: A report on an international workshop. *SPARC Newsletter,* No. 30, SPARC Office, Toronto, Ontario, Canada, 9–15.

Pierrehumbert, R. T., and R. Roca, 1998: Evidence for control of Atlantic subtropical humidity by large scale advection. *Geophys. Res. Lett.,* **25,** 4537–4540.

——, H. Brogniez, and R. Roca, 2007: On the relative humidity of the atmosphere. *The Global Circulation of the Atmosphere,* T. Schneider and A. H. Sobel, Eds., Princeton University Press, 400 pp.

Reynolds, R. W., N. A. Rayner, T. M. Smith, D. C. Stokes, and W. Wang, 2002: An improved in situ and satellite SST analysis for climate. *J. Climate,* **15,** 1609–1625.

Riehl, H., and J. S. Malkus, 1958: On the heat balance in the equatorial trough zone. *Geophysica,* **6,** 503–538.

Sherwood, S. C., 1996: Maintenance of the free-tropospheric tropical water vapor distribution. Part II: Simulation by large-scale advection. *J. Climate,* **9,** 2919–2934.

——, R. Roca, T. M. Weckwerth, and N. G. Andronova, 2010: Tropical water vapor, convection, and climate. *Rev. Geophys.,* **48,** RG2001, doi:10.1029/2009RG000301.

Soloviev, A., R. Lukas, and H. Matsuura, 2002: Sharp frontal interfaces in the near-surface layer of the tropical ocean. *J. Mar. Syst.,* **37,** 47–68.

Stephens, G. L., and Coauthors, 2002: The CloudSat mission and the A-Train: A new dimension of space-based observations of clouds and precipitation. *Bull. Amer. Meteor. Soc.,* **83,** 1771–1790.

Su, H., W. G. Reid, J. H. Jiang, J. W. Waters, D. L. Wu, and E. J. Fetzer, 2006: Enhanced positive water vapor feedback associated with tropical deep convection: New evidence from Aura MLS. *Geophys. Res. Lett.,* **33,** L05709, doi:10.1029/2005GL025505.

Susskind, J., C. Barnet, J. Blaisdell, L. Iredell, F. Keita, L. Kouvaris, G. Molnar, and M. Chahine, 2006: Accuracy of geophysical parameters derived from Atmospheric Infrared Sounder/Advanced Microwave Sounding Unit as a function of fractional cloud cover. *J. Geophys. Res.,* **111,** D09S17, doi:10.1029/2005JD006272.

Waliser, D. E., and N. E. Graham, 1993: Convective cloud systems and warm-pool sea surface temperatures: Coupled interactions and self-regulation. *J. Geophys. Res.,* **98,** 12 881–12 893.

Wang, J., D. J. Carlson, D. B. Parsons, T. F. Hock, D. Lauritsen, H. L. Cole, K. Beierle, and E. Chamberlain, 2003: Performance of operational radiosonde humidity sensors in direct comparison with a chilled mirror dew-point hygrometer and its climate implication. *Geophys. Res. Lett.,* **30,** 1860, doi:10.1029/2003GL016985.

Wu, D. L., J. H. Jiang, and C. P. Davis, 2006: EOS MLS cloud ice measurements and cloudy-sky radiative transfer model. *IEEE Trans. Geosci. Remote Sens.,* **44,** 1156–1165.

Zhang, C., B. E. Mapes, and B. J. Soden, 2003: Bimodality in tropical water vapour. *Quart. J. Roy. Meteor. Soc.,* **129,** 2847–2866.